Arbitrage-free Self-organizing Markets with GARCH Properties: Generating them in the Lab with a Lattice Model

B. Dupoyet[a,b], H.R. Fiebig[a,c,*], D.P. Musgrove[a,c]

[a] *Florida International University, Miami, Florida 33199, USA*
[b] *Department of Finance*
[c] *Department of Physics*

Abstract

We extend our studies of a quantum field model defined on a lattice having the dilation group as a local gauge symmetry. The model is relevant in the cross-disciplinary area of econophysics. A corresponding proposal by Ilinski aimed at gauge modeling in non-equilibrium pricing is realized as a numerical simulation of the one-asset version. The gauge field background enforces minimal arbitrage, yet allows for statistical fluctuations. The new feature added to the model is an updating prescription for the simulation that drives the model market into a self-organized critical state. Taking advantage of some flexibility of the updating prescription, stylized features and dynamical behaviors of real-world markets are reproduced in some detail.

Keywords: Econophysics, Financial markets, Statistical field theory, Self-organized criticality
PACS: 89.65.Gh, 89.75.Fb, 05.50.+q, 05.65.+b

1. Introduction

The analysis and modeling of financial price time series has a long history [1, 2, 3] and has attracted considerable interest at an accelerated pace in the last two decades. Technological advances have made it possible to collect and process vast amounts of data. As a result, various stylized facts about the statistics of financial data have been discovered [4, 5, 6]. These features are mostly concerned with scaling laws, akin to findings in many systems described by statistical physics. There, scaling behavior arises from the interaction of many units in such a way that a critical state is reached. Thus, one may ask if a financial market, for example, can be modeled based on similar principles. In generic terms, the building blocks could be many individual agents with suitable mutual interactions. Indeed, Lux and Marchesi have shown that scaling laws can arise in such a setting [7].

When building a microscopic model it is prudent to rely on a theoretical foundation supported by evidence. In the present work, we will employ two such principles. First, arbitrage opportunities will be annihilated during the time evolution of the market, though

*Corresponding author

admitting statistical fluctuations. Second, the dynamics of the model will drive it into a self-organized critical state, thus naturally giving rise to scaling behavior. Both aspects have been investigated separately in previous work, see [8] and [9] respectively. Here, we merge those elements into a microscopic market model, using numerical simulation to study its characteristics.

The next section gives an overview of the model's dynamics and definitions.

2. Lattice model

Following a proposal by Ilinski [10] we define a lattice field theory with a ladder topology as shown in Fig. 1. In physics terms there are matter fields $\Phi(x) \in \mathbb{R}^+$ defined on sites $x = (i, j)$, where $j = 0 \ldots n$ means discretized time, and $i = 0, 1$ is a spatial index. These are represented by filled circles in Fig. 1. In addition, there are gauge fields $\Theta_\mu(x) \in \mathbb{R}^+$ which live on links starting at site x in temporal $\mu = 0$ or spatial $\mu = 1$ direction. Those are represented by arrowed lines in Fig. 1.

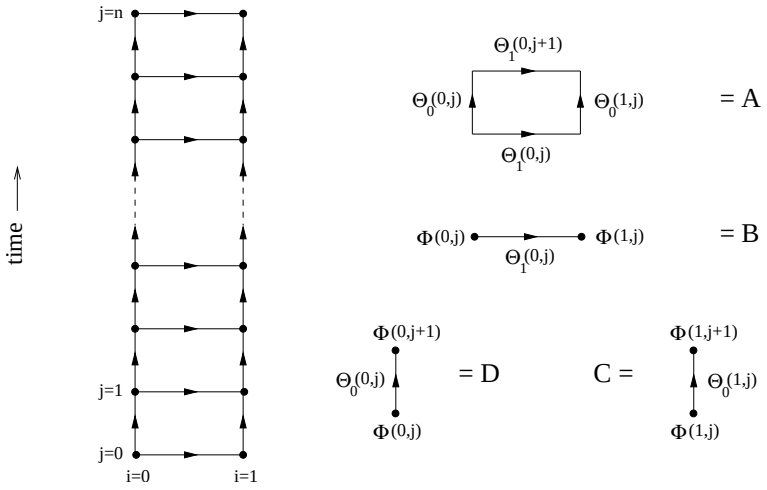

Figure 1: Left: Illustration of the ladder geometry of the lattice model and the label scheme for the fields. Right: Depiction of the gauge invariant elements A, B, C, D used in the action.

As a model for a financial market, again following [10], we interpret the matter field as instances of an account value, in some unit. At $i = 0$ it could be a cash account, whereas at $i = 1$ the value may be interpreted as the number of shares owned in some financial instrument. The spatial links $\Theta_1(0, j)$, connecting cash and shares, are simply conversion factors between the corresponding units. Temporal links $\Theta_0(0, j)$, which connect cash value sites one time step apart, mean interest rate factors. Similarly, temporal links $\Theta_0(1, j)$, starting from a shares site, carry information about the change in share value one time step apart.

The rationale behind such a model is to describe a market that dynamically evolves independent of the trading units being used. For example, in comparable markets, the dynamics should not depend on the specific, notably arbitrary, currency unit being used

in transactions. This, at least, is the hypothesis which should apply to markets trading in like instruments.

Mathematically, this idea is implemented by a quantum field theory with local gauge invariance. Such has been worked out in great detail in the context of financial markets [10]. In a previous work we have studied some aspects of those ideas using numerical simulation [8]. Since the current work is directly building on the latter, we refer the reader to [8] for the technical details. In particular, we shall use the nomenclature therein. However, to keep the presentation self contained, the essential building blocks are discussed in what follows.

The dynamics of the model derives from an action $S[\Theta, \Phi, \bar{\Phi}]$ for the lattice fields that is invariant with respect to local gauge transformations

$$\begin{aligned} \Phi(x) &\rightarrow g(x)\Phi(x) && (1)\\ \bar{\Phi}(x) &\rightarrow \bar{\Phi}(x)g^{-1}(x) && (2)\\ \Theta_\mu(x) &\rightarrow g(x)\Theta_\mu(x)g^{-1}(x+e_\mu)\,, && (3) \end{aligned}$$

where $\bar{\Phi}(x) = 1/\Phi(x)$ and $g(x) \in G$ is an element of the dilation group $G = \mathbb{R}^+$, i.e. multiplication by positive real numbers. Those carry out conversions between (arbitrary) units. The action is constructed from the elements depicted in Fig. 1. These are the smallest gauge invariant objects that can be assembled from the fields.

The diagram associated with label A is known as the elementary plaquette

$$P_{\mu\nu}(x) = \Theta_\mu(x)\Theta_\nu(x+e_\mu)\Theta_\mu^{-1}(x+e_\nu)\Theta_\nu^{-1}(x)\,. \tag{4}$$

Its value is interpreted as the gain (or loss) realized through an arbitrage move [10]. The global minimum of the classical action $S[\Theta, \Phi, \bar{\Phi}]$ corresponds to zero arbitrage [8]. Quantization of the field is done through the usual path integral formalism. The partition function thus is defined as the functional integral

$$Z(\beta) = \int [D\Theta][D\Phi] e^{-\beta S[\Theta, \Phi, \bar{\Phi}]}\,. \tag{5}$$

In this way stochastic fluctuations about zero arbitrage are allowed. Their magnitude is regulated by the parameter β.

Diagrams B,C,D are gauge invariant elements of the form

$$R_\mu(x) = \bar{\Phi}(x)\Theta_\mu(x)\Phi(x+e_\mu)\,, \tag{6}$$

where e_μ is a unit vector in direction μ. Diagram C, for example, gives the value of the investment instrument at time $j+1$ divided by its value at j, provided we adopt the above interpretation of the fields. It is a measure for the relative change of the asset value during one time step

$$R_0(1,j) = \bar{\Phi}(1,j)\Theta_0(1,j)\Phi(1,j+1)\,. \tag{7}$$

We also define the related quantity

$$r_{j+1} = \log R_0(1,j)\,, \tag{8}$$

commonly called the 'return', indicating a gain (> 0) or a loss (< 0) at the end of the time step.

3. Updating strategy

The generation of lattice field configurations as implemented in [8] follows a standard procedure. Based on the action $S[\Theta, \Phi, \bar{\Phi}]$ the field components are updated through a heatbath algorithm [11, 12] linked to the partition function (5). Periodic boundary conditions (in the time direction) are imposed on all fields as well. However, in contrast to [8], the updating strategy is modified in two respects.

First, we do set constraints on the fields that live on the axis $i = 0$, see Fig. 1. The reasoning here is that we wish to design the model such that the axis describes a cash account subject to accumulating interest. The interest rate is endogenously determined. Even at 10% annually the daily rate factor is 1.0003 and thus hardly distinguishable from one. As the model is designed to describe a high frequency market, where the time extent n translates to typically a day, or so, we wish to set a constraint accordingly. In a gauge model this is not straightforward, because the meaning of the field components is gauge dependent. To remedy this situation, gauge fixing is called for. With reference to (1-3) define a gauge transformation along the axis $i = 0$,

$$g(0, j) = \bar{\Phi}(0, j)\,, \tag{9}$$

with $g(x)$ on all other sites being arbitrary. The gauge transformed fields along the axis, $i = 0$, then are

$$\begin{aligned} \Phi'(0, j) &= g(0, j)\Phi(0, j) = 1 && (10)\\ \bar{\Phi}'(0, j) &= \bar{\Phi}(0, j)g^{-1}(0, j) = 1 && (11)\\ \Theta'_0(0, j) &= \bar{\Phi}(0, j)\Theta_0(0, j)\Phi(0, j + 1) = R_0(0, j)\,. && (12) \end{aligned}$$

In the last equation we recognize the link variable as the (gauge invariant) return (6) of the cash holding during one time step. We therefore set

$$\Theta'_0(0, j) = 1\,. \tag{13}$$

In our simulation we choose a random start for the lattice fields. From there, the constraint $R_0(0, j) = 1$ is then implemented by applying the gauge transformation (9), and then setting the axis links to one (13). During the subsequent updating procedure the axis fields $\Phi(0, j)$ and $\Theta_0(0, j)$ are never changed. Nonetheless, the right-hand side of (13) may differ from one, depending on the interest rate factor desired.

The next step is to run a heatbath algorithm with the lattice action $S[\Theta, \Phi, \bar{\Phi}]$ until equilibrium is reached [8]. The lattice field configurations then model a market environment where arbitrage opportunities exist only briefly, subject to fluctuations due to the quantum nature of the fields. In economic terms this model describes an efficient market. Equilibrium, however, does not seem to be realized in the real world [13].

Second, subscribing to this paradigm, we introduce a new element which is applied post equilibrium. In [9] we have studied a simple model where market instances live along a linear chain in time direction. The sites carry fields $r_j \in \mathbb{R}^+$ which are directly interpreted as returns, thus having the same meaning as (8). There is no gauge field in the simple model. The key ingredient is an updating algorithm that mimics the popular Bak Sneppen evolutionary model [14, 15, 16]. The quantity

$$v_j = r_j(r_{j+1} - r_{j-1}) \tag{14}$$

turned out to be essential to the field dynamics. In the context of [9] the updating strategy consists in finding the site j_s for which the absolute value of (14) is maximal $|v_{j_s}| = \max\{|v_j| : j = 0 \dots n\}$, and then replace r_{j_s} and its neighbors $r_{j_s \pm 1}$ with random numbers. Iterating this process leads to a self-organized critical state and produces price times series, and related statistics, which are almost indistinguishable from those in real markets [8].

In view of those results it seems desirable to replicate this updating strategy within the framework of the gauge model as closely as possible. Towards this end, we still do define the 'fitness' measure v_j as in (14), however, the returns are now given by (8), and (7). Their composition is illustrated in Fig. 2. The updating prescription proceeds with finding the 'signal'

$$V = \max\{|v_j| : j = 1 \dots n\} \tag{15}$$

of the field configuration, and the site j_s of its location

$$|v_{j_s}| = V \,. \tag{16}$$

We then update the three field components $\Phi(1, j_s - 1), \Theta_0(1, j_s - 1), \Phi(1, j_s)$, which enter the return r_{j_s}, and the two next-neighbor links $\Theta_0(1, j_s), \Theta_0(1, j_s - 2)$, see Fig. 2. Note that $\Phi(1, j_s + 1)$ and $\Phi(1, j_s - 2)$ are left unchanged. In this way only the three returns $r_{j_s - 1}, r_{j_s}, r_{j_s + 1}$ are affected. This strategy most closely resembles the updating prescription used in [8].

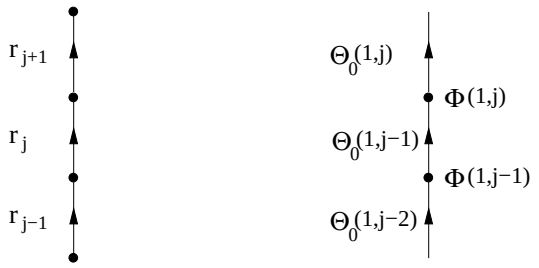

Figure 2: Left: Illustration of the returns involved in the 'fitness' criterion (14) (left), and the field components subject to updating (right), done at the 'signal' site $j = j_s$.

Updating those field components consists in drawing random numbers from certain probability distributions. We have chosen those based on the lattice action $S[\Theta, \Phi, \bar{\Phi}]$ mentioned above. Heatbath steps using the corresponding Boltzmann-like distribution, see (5), are applied to the various field components. Essentially, the probability distribution for a given field component is given by its local environment. It is convenient to rewrite the fields as

$$\Theta_\mu(x) = e^{\theta_\mu(x)} \quad \text{and} \quad \Phi(x) = e^{\phi(x)} \,. \tag{17}$$

Then, after a gauge transformation, the probability densities for the gauge fields and the matter fields, respectively, have the form

$$p_\Theta(\theta_\mu(x)) \;\propto\; \exp(-2\beta\sqrt{L_\Theta \bar{L}_\Theta}\cosh(\theta_\mu(x)))\,) \tag{18}$$

$$p_\Phi(\phi(x)) \;\propto\; \exp(-2\beta\sqrt{L_\Phi \bar{L}_\Phi}\cosh(\phi(x)))\,) \,. \tag{19}$$

These results are derived in detail in Appendix Appendix A. The coefficients $L_\Theta, \bar{L}_\Theta$ and $L_\Phi, \bar{L}_\Phi$ are independent of $\Theta_\mu(x)$ and $\Phi(x)$, respectively. The products $L_\Theta \bar{L}_\Theta$ and $L_\Phi \bar{L}_\Phi$ are gauge invariant and, together with the parameter β, determine the variance of the probability distributions for the field components. Those distributions strongly depend on the local environment at the location of the fields.

Now, at each updating step we randomly draw fields $\phi'(1,j)$, $j_s - 1 \leq j \leq j_s$, from (19). Relevant averages considered are

$$a_\theta = \frac{1}{3} \sum_{j=j_s-2}^{j_s} \theta_0(1,j) \quad \text{and} \quad a_\phi = \frac{1}{2} \sum_{j=j_s-1}^{j_s} \phi'(1,j)\,. \tag{20}$$

Updating the fields then is accomplished by replacing

$$\theta_0(1,j) \quad \longleftarrow \quad \theta_0(1,j) - \chi a_\theta\,, \quad j_s - 2 \leq j \leq j_s \tag{21}$$

$$\phi(1,j) \quad \longleftarrow \quad \phi'(1,j) - a_\phi\,, \quad j_s - 1 \leq j \leq j_s\,. \tag{22}$$

By including the parameter χ we have introduced a novel feature to the updating process. While $\chi = 1$ essentially mirrors the strategy in [9], deviations from that value introduce very interesting features to the model. We will be able to describe a range of different returns distributions and time series, as will be described in the next section.

Finally, we apply heatbath updates to the two spatial (horizontal) link variables $\theta_1(0,j)$, $j_s - 1 \leq j \leq j_s$, which connect to the affected matter fields, see (22). These links occur in three elementary plaquettes

$$P_{10}(0,j-1) = \Theta_1(0,j-1)\Theta_0(1,j-1)\Theta_1^{-1}(0,j)\Theta_0^{-1}(0,j-1)\,, \tag{23}$$

see (4), where $j_s - 1 \leq j \leq j_s + 1$. The reason is that updating $\theta_0(1,j)$, as prescribed by (21), changes the plaquettes (23) and thus upsets the no-arbitrage environment of the lattice fields. Updating the above links with the lattice action $S[\Theta, \Phi, \bar{\Phi}]$ rectifies this circumstance.

4. Results

The simulations were done on a lattice of size $n = 782$ with gauge field coupling parameter $\beta = 1$, and the matter field couplings $d_\mu^\pm = \bar{d}_\mu^\pm = 1$. These parameters are the same as in [8], with the one asset model $m = 1$. The number of heatbath update steps was 10^4 to equilibrate the field from a random start. Final configurations were reached after 4×10^6 'signal' updates.

First, we discuss the effect of the parameter χ in (21). A suitable observable (order parameter) is the gauge invariant link along the asset axis (7). Using the notation (17) we have

$$R_0(1,j-1) = \exp\left(-\phi(1,j-1) + \theta_0(1,j-1) + \phi(1,j)\right) = \exp(r_j)\,. \tag{24}$$

The updating algorithm, described in Sect. 3, employs symmetric probability distribution functions for θ and ϕ. Consequently, the probabilities for realizing a gain $r_j > 0$ and a loss $r_j < 0$ are equal. Thus we define the symmetric link

$$L_j = \frac{1}{2}\left(\exp(r_j) + \exp(-r_j)\right) - 1 = \cosh(r_j) - 1 \tag{25}$$

and its lattice average

$$L = \frac{1}{n}\sum_{j=1}^{n} L_j \,. \tag{26}$$

Numerically, the value of L is particular to a distinct lattice field configuration. We denote the (stochastic) average over field configurations with angle brackets, here $\langle L\rangle$. In Fig. 3 the dependence of $\langle L\rangle$ on the parameter χ is displayed. The plot symbols '$\bullet$' indicate data points from simulations at $\chi = 10^k, k = -6, -5 \ldots + 1$. The errors come from 48 field configurations. The line curve in Fig. 3 is a four parameter fit, $a_1 \ldots a_4$, to those eight data points with $y = a_1 \tanh[a_2(-\log_{10}(x) + a_3)] + a_4$. Remarkably, there clearly is a transition region in the, approximate, range $10^{-4} < \chi < 10^{-1}$. For small values $\chi \ll 10^{-4}$ the average link operator saturates at 0.2406, while for large values $10^{-1} \ll \chi$ it tends to 0.0092, according to the fit. Using the (crude) conversion $\cosh(r) - 1 = L$ for simplicity, see (25), this corresponds to returns $r \approx \pm 0.68$ and $r \approx \pm 0.14$, respectively, for the above limits of χ. Those limits may describe valid markets, which could be seen as volatile and calm, respectively. In view of this observation the transition region becomes particularly interesting. It opens up the possibility to simulate markets with a wide range of features between those extremes. Below, we will present results for $\chi = 0.0005, 0.0013$ within the transition region. Those are indicated by plot symbols '+' in Fig. 3.

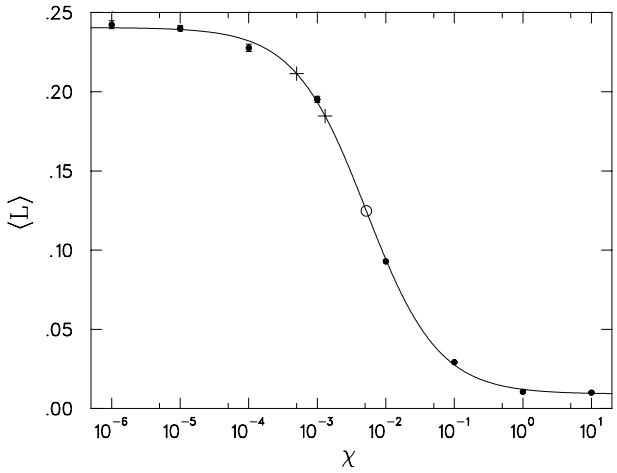

Figure 3: Expectation value $\langle L\rangle$ of the gauge invariant average link operator (26) as a function of the update parameter χ in (21). The plotting symbols '$\bullet$' and '+' correspond to specific values of χ for which simulations were made. The symbol '$\circ$' indicates the symmetry point $\chi = 0.0052$ of the fit.

During a simulation, the evolution of the lattice towards a critical state can be monitored, for example, by observing the signal V, see (15), as a function of the updating step counter, say $s = 0, 1, 2 \ldots$. Writing $V(s)$ we follow [16] and define the 'gap' function

$$G(x) = \min\{V(s) : s \in \mathbb{N} \cup \{0\} \text{ and } s \le x\} \quad \text{with} \quad x \in \mathbb{R}^+ \cup \{0\} \,. \tag{27}$$

This is a decreasing piecewise constant function with discontinuities at certain discrete values $x_k, k \in \mathbb{N}$. The set of update steps between x_{k-1} and x_k is called an avalanche of length $\Lambda_k = x_k - x_{k-1}$. Eventually, as $x \to \infty$, the avalanche size diverges and the

system has reached criticality [16]. For an elaboration on these concepts, presented in a context close to the current work, we refer the reader to [9]. We here only show a key result.

In Fig. 4 the frequency distribution $\Delta N/\Delta\Lambda$ of the avalanche sizes is displayed. Here $\Delta\Lambda$ is a binning interval for the avalanche sizes and ΔN is the count of avalanches within that interval. We have used 10000 bins with $\Delta\Lambda = 1$. The data points and errors come from an ensemble average over 2400 independent lattice simulations with 4×10^6 update steps each. The log-log plot clearly shows power law behavior. A power law indicates scaling, which is a signature feature of a critical system.

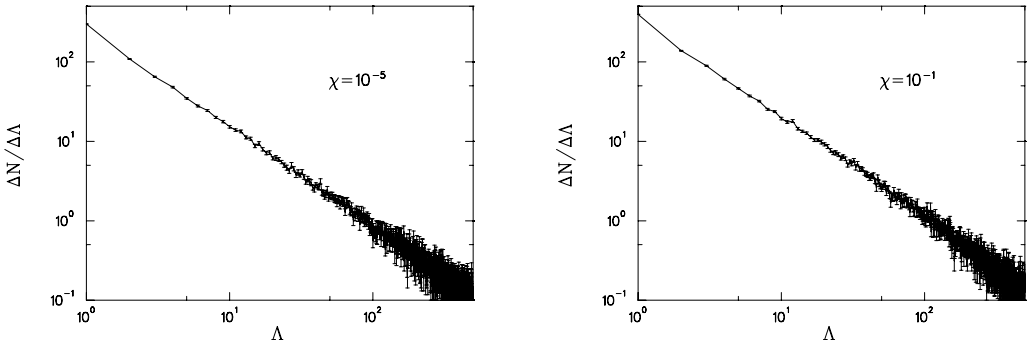

Figure 4: Frequency distributions of avalanche sizes for two values $\chi = 10^{-5}, 10^{-1}$ of the update parameter.

For the time being, we continue to present results for the two update parameters $\chi = 10^{-5}$ and $\chi = 10^{-1}$. These values correspond to the boundaries of the transition region, see Fig. 3. Inside that region, the frequency distributions of avalanche sizes are almost indistinguishable from the results shown in Fig. 4. Examples of model markets for suitable update parameters in the transition region are discussed below.

The gains distributions produced by the lattice model with $\chi = 10^{-5}, 10^{-1}$ are shown in Fig. 5. The gauge invariant returns r, as defined in (8), are put into bins of size Δr, and $\Delta c/\Delta r$ is the number of counts per bin. The errors are obtained from 2400 independent simulations. While both histograms possess fat tails, we observe a distinct difference of the qualitative features for the distributions. At $\chi = 10^{-5}$ a distinctly pointed central peak sits on very broad bulging tails. Looking at $\chi = 10^{-1}$ the central peak has broadened such that its very top is almost Gaussian while the tails look linear. This means that the two distributions cannot be mapped into each other by simple scale transformations applied to the axes. The two gains distributions describe genuinely different markets. Interestingly, this matches our previous assessment of the the regions $\chi \ll 10^{-5}$ and $10^{-1} \ll \chi$ discussed in the context of Fig. 3.

Examples of returns time series for each of the two parameters χ are displayed in Fig. 6. By visual inspection, both of those exhibit volatility clustering, yet display different dynamical behavior. In the realm of $\chi = 10^{-5}$ the time series appears to favor one side of the zero mark for short periods of time, as compared to the series of $\chi = 10^{-1}$ which smoothly fluctuates about zero in either direction.

For a closer investigation, we have selected the parameters $\chi = 0.0005, 0.0013$ from the transition region. In Fig. 3 their locations are marked by '+' plot symbols. The

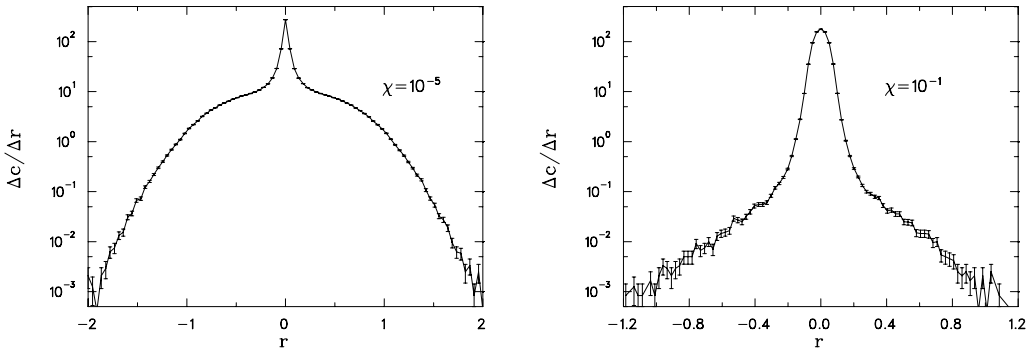

Figure 5: Lattice generated gains distributions of the returns r for the values $\chi = 10^{-5}, 10^{-1}$ of the update parameter.

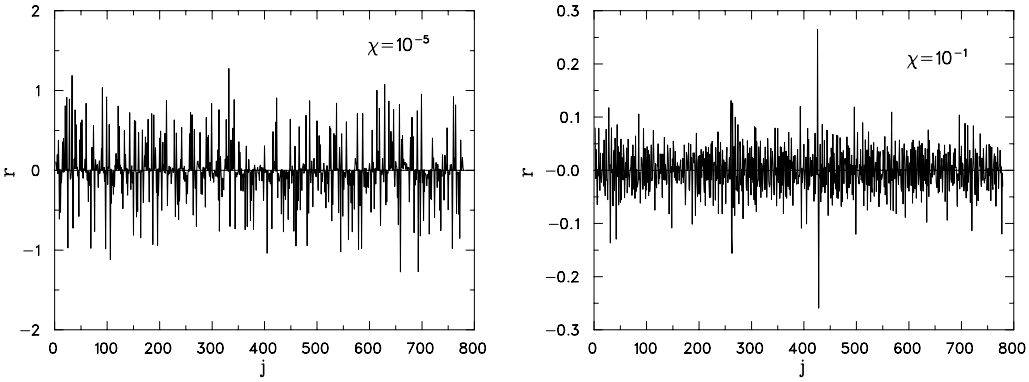

Figure 6: Examples of returns time series r_j versus the lattice time j at $\chi = 10^{-5}$ and $\chi = 10^{-1}$.

choice of these values reflects our observation that model market characteristics, say the gains distribution for example, hardly change as χ is decreased from ≈ 0.1 to ≈ 0.005. Most of the market model tuning happens in the upper segment of the $\langle L \rangle$ curve in Fig. 3 as χ further decreases below ≈ 0.005.

It is tempting to utilize this range for modeling historical markets of varying characteristics. However, we leave this to future work. Here, our focus is on the properties of time series dynamics of the lattice model as being evaluated with standard financial analysis tools.

The gains distributions for $\chi = 0.0005$ and $\chi = 0.0013$ are displayed in Fig. 7. They were obtained from 2400 simulation runs with length 4×10^6 each. Again, the distributions clearly exhibit fat tails but are otherwise different in their shapes. The $\chi = 0.0005$ distribution puts more emphasis on larger returns than the $\chi = 0.0005$ distribution. This is echoed in the corresponding returns time series.

Samples of those time series are displayed in Fig. 8 for $\chi = 0.0005$ and Fig. 9 for $\chi = 0.0013$, respectively. Each figure is composed of eight randomly selected independent simulation runs with 4×10^6 updates each. Compared to the $\chi = 0.0013$ time series, the $\chi = 0.0005$ series have a, somewhat perceptible, higher occurrence of volatility clusters

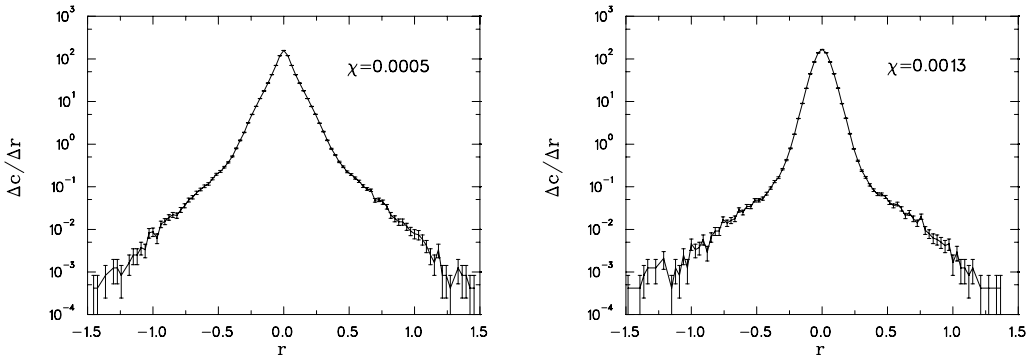

Figure 7: Gains distributions from simulations with update parameter $\chi = 0.0005$ and $\chi = 0.0013$.

as well as bigger swings between them.

We now turn to gauging the ability of our model to replicate various features of financial markets. One crucial aspect of financial markets returns is their volatility, as well as how this volatility evolves over time. Volatility is more relevant today than ever, with large spikes possibly occurring in short periods of time. Financial markets returns generally display volatility 'clusters'. These clusters indicate that once the volatility is high, it tends to remain high for a while, and that similarly, once it has come down, it tends to remain low for some time. A convenient and well-accepted way of modeling such characteristics is through the use of the Auto Regressive Conditional Heteroskedasticity (ARCH) model pioneered by Engle [2] or through the use of the more encompassing Generalized Regressive Conditional Heteroskedasticity (GARCH) model proposed by Bollerslev [3].

Whether working on pricing a derivative product, attempting to hedge an exposure, optimizing a portfolio in a mean-variance framework, or estimating the Value-At-Risk of a position, the ability to capture and model the stochasticity and the clustering properties of the volatility is paramount. Not doing so can lead to the wrong probability distribution being used, since volatility clusters impact the shape of returns distributions in two important ways. First, the fact that a period of calm statistically tends to be followed by another period of calm indicates that there will be a fairly large amount of probability mass around the mean (return). Graphically this phenomenon translates into a probability distribution function that is higher than the Gaussian one in the vicinity of the mean. Second, the fact that a period of extreme movements statistically tends to be followed by another period of extreme movements indicates that there will be non-negligible amounts of probability mass in the tails areas. Graphically this phenomenon translates into a probability distribution function that is higher than the Gaussian one in the vicinity of the tails.

The fairly wide-ranging GARCH specification models the volatility as both a function of past squared return shocks and of past levels of itself. If both past return shocks and past volatility levels are low, for instance, the odds are that the next volatility levels will remain low. If past volatility levels are low but recent past return shocks are high, the levels of volatility will likely increase. If past volatility levels are high but recent past return shocks are low, the levels of volatility will perhaps decrease. Finally, if both past

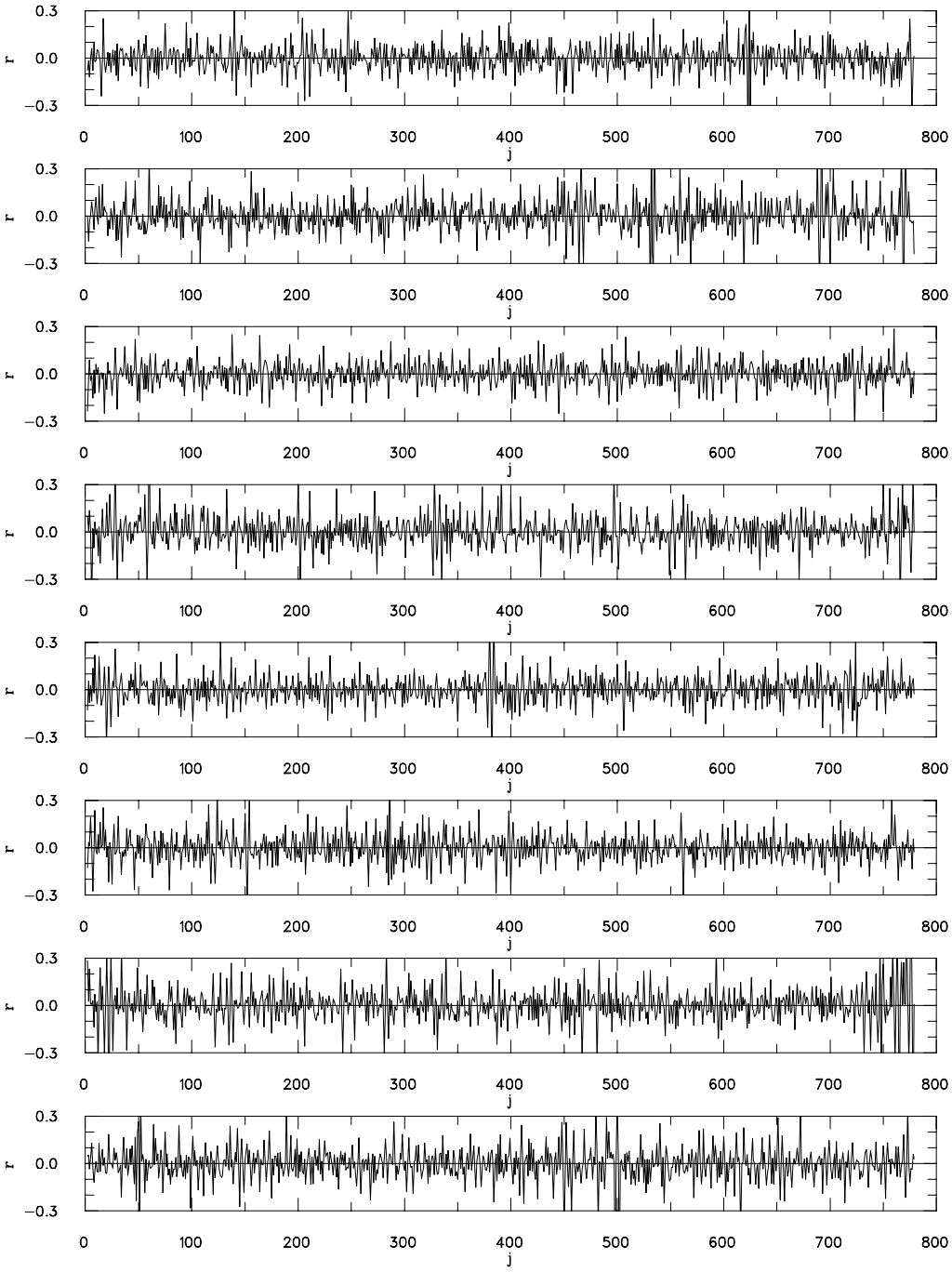

Figure 8: Samples of returns time series for the update parameter $\chi = 0005$. The corresponding gains distribution is shown in Fig. 7.

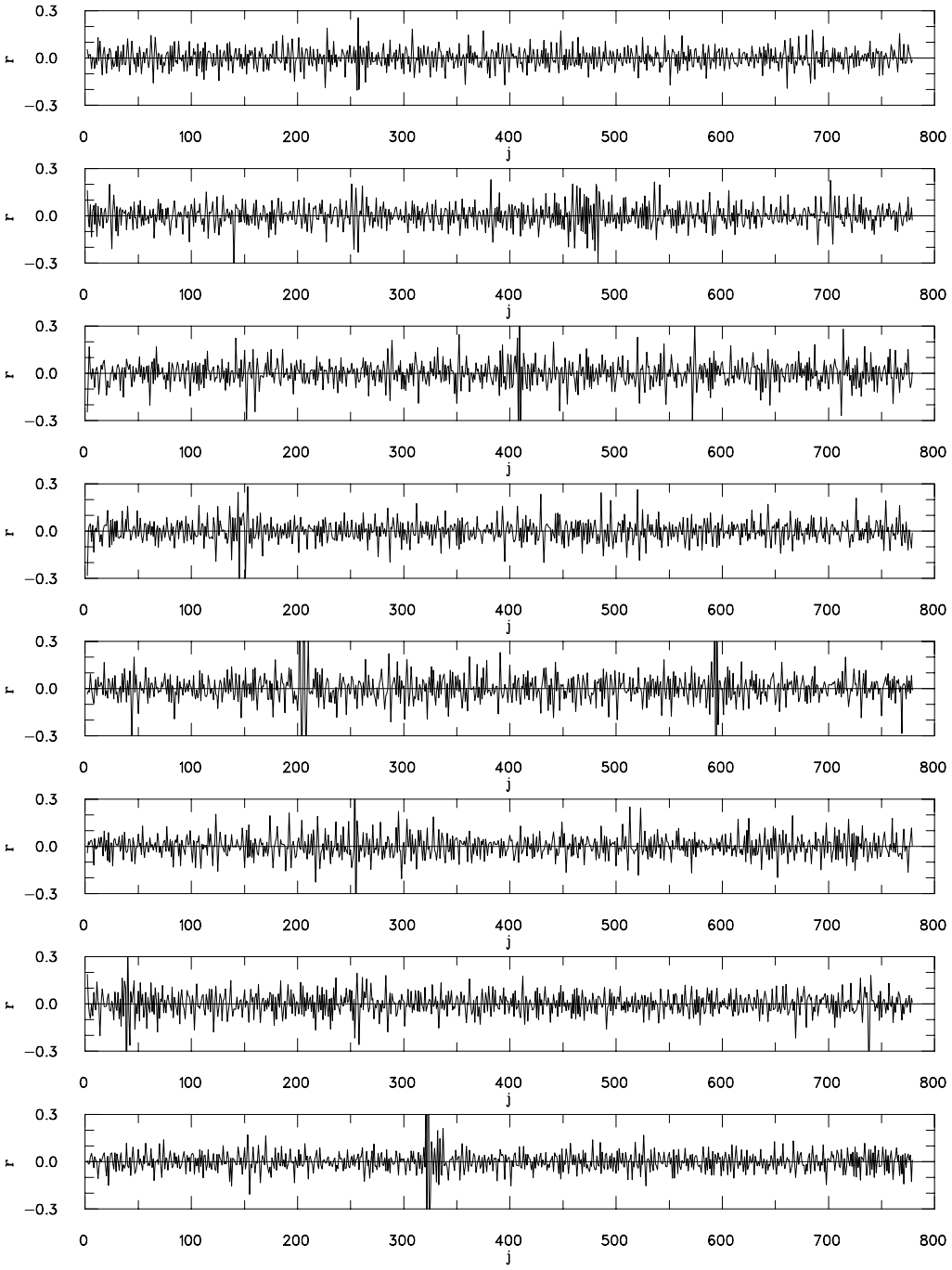

Figure 9: Samples of returns time series for the update parameter $\chi = 0013$. The corresponding gains distribution is shown in Fig. 7.

return shocks and past volatility levels are high, the odds are that the next volatility levels will remain high. In a GARCH(p,q) specification, the number of lags p and q allowed for past shocks and past volatility levels are limitless. However, Hansen and Lunde [17] explore the ability of 330 different ARCH/GARCH models to capture the features of various financial returns and come to the conclusion that a GARCH(1,1) model performs just as well as the more 'sophisticated' ones. Our specification for the volatility σ_t^2 at time t is thus a GARCH(1,1) described by the following equation:

$$\sigma_t^2 = \alpha_0 + \alpha_1 \epsilon_{t-1}^2 + \beta_1 \sigma_{t-1}^2 \,, \tag{28}$$

where ϵ_{t-1}^2 and σ_{t-1}^2 are the one-period lagged squared return shock and one-period lagged variance, respectively.

We simulate 100 lattice time series for two different levels of our tuning parameter χ. In the first set of simulations, χ is set equal to a value of 0.0005 while in our second set of simulations, χ is set equal to a value of 0.0013. This allows for the generation of different returns distributions and times series, namely financial markets returns with varying degrees of activity: The set of simulations using a χ value of 0.0005 reflect a somewhat more volatile market than the set of simulations using a χ value of 0.0013. Previous studies have shown that even a simple lattice model [9] is able to produce returns volatility dynamics displaying some ARCH/GARCH effects, and also that it is able to produce returns volatility dynamics that are rather consistent with those of NASDAQ historical returns. With the present model, we are here conducting a more extensive investigation: We estimate GARCH(1,1) fits from a large number of randomly chosen lattice configurations for the purpose of demonstrating the stability, consistency, and flexibility of our lattice model.

The resulting parameters obtained are shown in Fig. 10 and in Fig. 11 for $\chi = 0.0005$ and $\chi = 0.0013$ respectively, for a total of 200 different lattice time series. For visual ease, the parameters are ordered before being plotted. In Fig. 10 one can thus immediately see that the β_1 parameter is between 0.85 and 1.0 in about 95% of the cases, a result consistent with Nasdaq GARCH(1,1)-estimated figures in [9]. In Fig. 11 the β_1 parameter is between 0.85 and 1.0 in about 80% of the cases. This indicates that the lagged volatility feedback is strongly consistent across various market conditions and various simulations. In Fig. 10 one can also see that the α_1 parameter is below 0.15 in about 99% of the cases, a result also consistent with Nasdaq GARCH(1,1)-estimated figures in [9]. Finally, in Fig. 11 the α_1 parameter is below 0.15 in about 99% of the cases, although a higher proportion is above 0.05 when compared to the values it takes in Fig. 10. These results indicate that the lagged return shock feedback is also strongly consistent across various market conditions and various simulations. The α_0 parameter is consistently very low in both cases, as it should at these high frequencies.

It is also interesting to note that for each parameter, we obtain some 'outliers' in about 5% to 20% of the cases, although they are outliers only in the sense that they differ from the other 95% to 80% of the estimates that are themselves incredibly consistent, and are not outliers in the sense that their values would be considered too extreme or unreasonable. It is important to note that when running multiple simulations, one is bound to obtain some results that differ somewhat from the estimates' consensus. For instance, even if one was to simulate an exact GARCH(1,1) process many times and subsequently estimate the parameters from the simulated data, some percentage of the

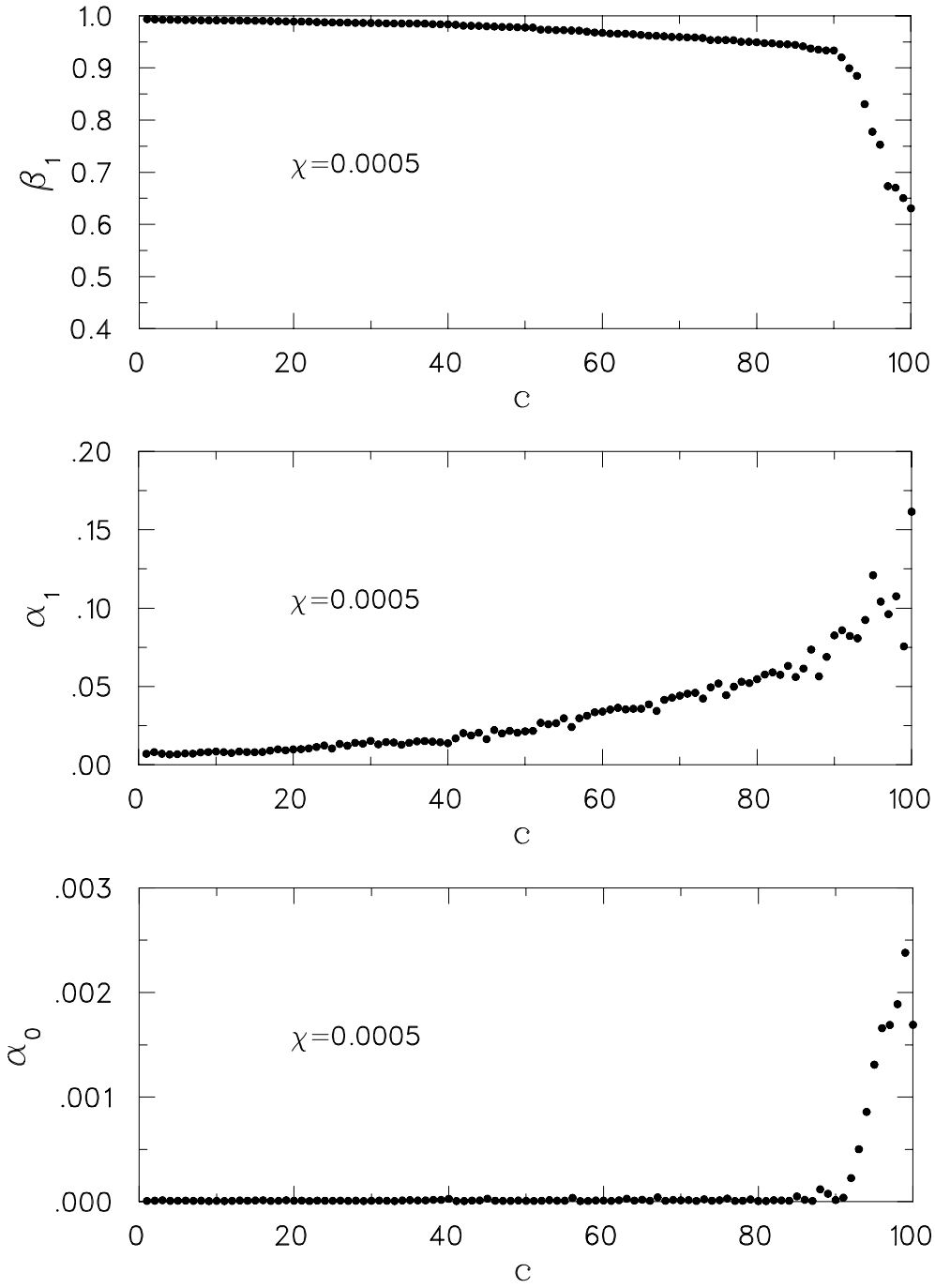

Figure 10: GARCH(1,1) fit parameters for a sample of 100 lattice time series at $\chi = 0.0005$. The configuration counter c has been subject to sorting with respect to β_1.

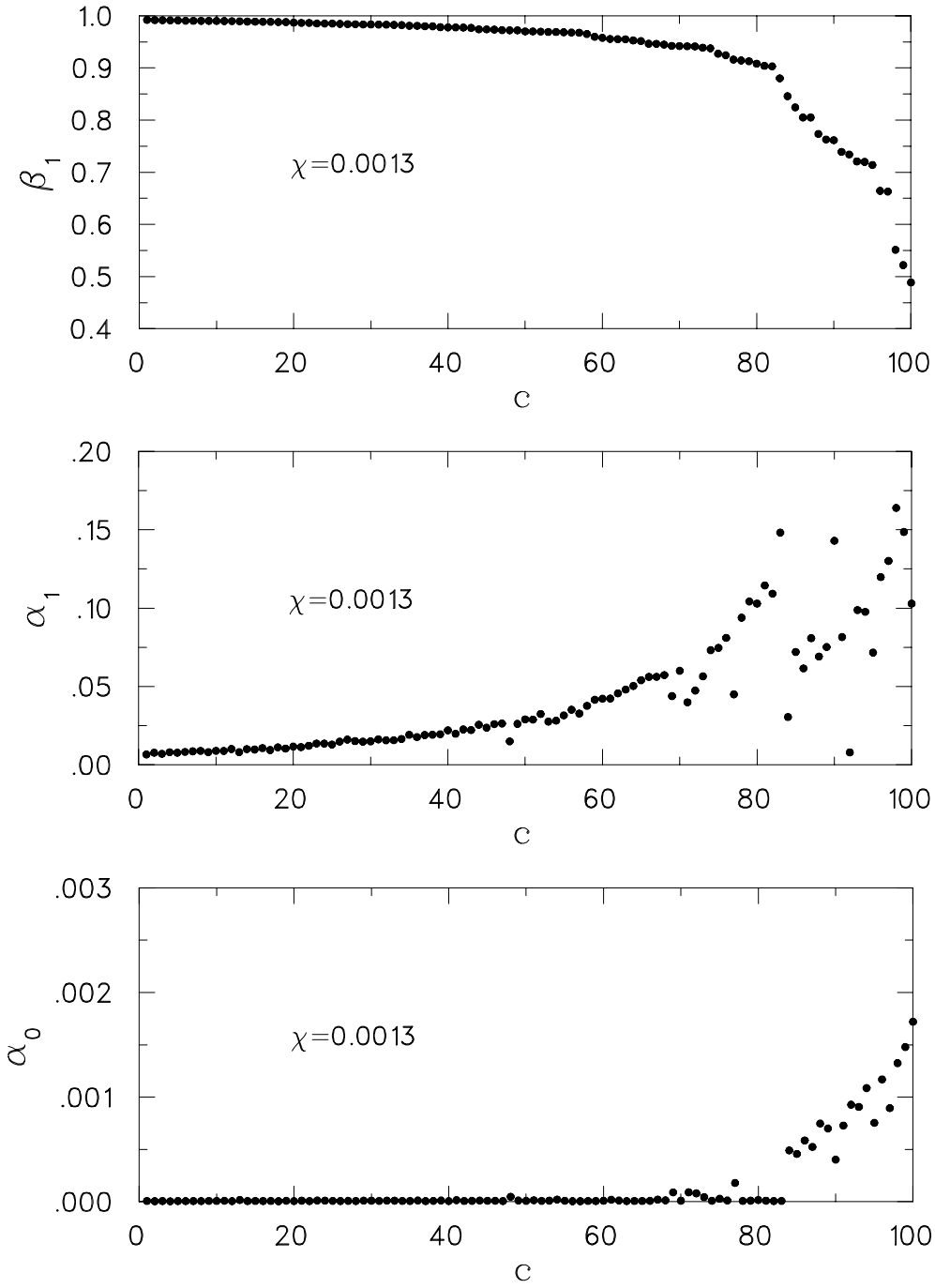

Figure 11: GARCH(1,1) fit parameters for a sample of 100 lattice time series at $\chi = 0.0013$. The configuration counter c has been subject to sorting with respect to β_1.

estimated parameters would stray from the median estimates. In summary, 100% of our estimated parameters are sensible, across various market conditions (more or less volatile) and thus across varying returns distributions, and over a myriad of simulations.

5. Conclusion

The subject of this work has been to explore a class of models designed to simulate the properties of financial markets. The output of the model is a time series of returns, from which gains distributions and related features could be derived. The potential of the model for replicating market dynamics, as described by standard financial analysis tools, was the primary aim of this study.

The production of our time series has been done by numerical simulation based on a lattice description of fields in time-asset space. We have restricted ourselves to a one-asset model linked to an interest rate account. The dynamics are based on a gauge invariant lattice action which, when quantized, gives rise to eliminating arbitrage opportunities up to stochastic fluctuations, thus reflecting real market conditions. The second pillar of the model is an updating prescription that evolves the lattice fields into a self-organizing critical state. This appears to be an essential element for reproducing certain stylized features of real markets.

As a third feature, a parameter has been introduced as a tuning tool, through which a variety of market characteristics, ranging from quiescent to volatile markets, can be modeled.

An extensive analysis of a very large number of time series features evaluated by a GARCH(1,1) analysis was performed. It turns out that close to 100% of the lattice model-generated time series give rise to sensible analysis parameters, rendering the model results almost indistinguishable from historical market data. In particular we could verify this observation across various market conditions and varying returns distributions.

We conclude that the model shows promise as a modeling tool for financial time series and look forward to further development and applications.

Appendix A. Gauge fixing

In the notation of [8], the probability density for a particular gauge field component has the form

$$p_\Theta(\theta_\mu(x)) \propto \exp(-\beta(\bar{L}_\Theta \exp(\theta_\mu(x)) + \exp(-\theta_\mu(x))L_\Theta)\,) \tag{A.1}$$

where L_Θ and $\bar{L}_\Theta$ are positive coefficients independent of $\theta_\mu(x)$. They reflect the (local) environment of the link variable. Under a gauge transformation, writing

$$g(x) = e^{h(x)}\,, \tag{A.2}$$

we have

$$\theta_\mu(x) \;\rightarrow\; \theta'_\mu(x) = h(x) + \theta_\mu(x) - h(x+e_\mu) \tag{A.3}$$

$$L_\Theta \;\rightarrow\; L'_\Theta = e^{h(x)} L_\Theta e^{-h(x+e_\mu)} \tag{A.4}$$

$$\bar{L}_\Theta \;\rightarrow\; \bar{L}'_\Theta = e^{h(x+e_\mu)} \bar{L}_\Theta e^{-h(x)}\,. \tag{A.5}$$

The transformation laws for L_Θ and $\bar{L}_\Theta$ can be derived directly by an examination of the lattice action $S[\Theta, \Phi, \bar{\Phi}]$. They are also obvious from the fact that the action is gauge invariant and the arguments of the exponential functions of (A.1) are made up from invariant contributions to it. We now choose the gauge transformation by requiring the new coefficients to be equal

$$\frac{L'_\Theta}{\bar{L}'_\Theta} = e^{2h(x)} \frac{L_\Theta}{\bar{L}_\Theta} e^{-2h(x+e_\mu)} = 1\,, \tag{A.6}$$

or

$$h(x+e_\mu) - h(x) = \frac{1}{2} \log(\frac{L_\Theta}{\bar{L}_\Theta})\,. \tag{A.7}$$

A solution of (A.7) is

$$h(x+e_\mu) = \frac{\lambda+1}{4} \log(\frac{L_\Theta}{\bar{L}_\Theta}) \tag{A.8}$$

$$h(x) = \frac{\lambda-1}{4} \log(\frac{L_\Theta}{\bar{L}_\Theta})\,, \tag{A.9}$$

where λ is a real parameter[1]. On all other sites, besides x and $x+e_\mu$, the gauge transformation function $h(x)$ is arbitrary. (For definiteness one may choose it to be zero.) In the new gauge, using (A.6), we have

$$\bar{L}'_\Theta e^{\theta'_\mu(x)} + e^{-\theta'_\mu(x)} L'_\Theta = 2\sqrt{L'_\Theta \bar{L}'_\Theta} \cosh(\theta'_\mu(x))\,. \tag{A.10}$$

Thus, the probability distribution function is

$$p'_\Theta(\theta'_\mu(x)) \propto \exp(-2\beta\sqrt{L'_\Theta \bar{L}'_\Theta} \cosh(\theta'_\mu(x)))\,. \tag{A.11}$$

Dropping the primes gives (18). Citing $L_\Theta \bar{L}_\Theta = L'_\Theta \bar{L}'_\Theta$, we note that the variance of the the probability distribution function is not altered by the gauge transformation.

Again, in the notation of [8], the probability density for a particular matter field component has the form

$$p_\Phi(\phi_\mu(x)) \propto \exp(-\beta(\bar{L}_\Phi \exp(\phi_\mu(x)) + \exp(-\phi_\mu(x)) L_\Phi)) \tag{A.12}$$

where L_Φ and $\bar{L}_\Phi$ are positive coefficients independent of $\phi_\mu(x)$, reflecting the (local) environment of the field variable. In this case, changing the gauge (A.2) entails the transformations

$$\phi(x) \rightarrow \phi'(x) = h(x) + \phi(x) \tag{A.13}$$

$$L_\Phi \rightarrow L'_\Phi = e^{h(x)} L_\Phi \tag{A.14}$$

$$\bar{L}_\Phi \rightarrow \bar{L}'_\Phi = \bar{L}_\Phi e^{-h(x)}\,. \tag{A.15}$$

[1]It may be used to control the effect of the gauge transformation on the matter fields $\phi(x)$ and $\phi(x+e_\mu)$.

The requirement $L'_\Phi/\bar{L}'_\Phi = 1$ leads to

$$h(x) = -\frac{1}{2}\log(\frac{L_\Phi}{\bar{L}_\Phi})\,, \tag{A.16}$$

while the gauge function is arbitrary on all sites other than x. Proceeding in the manner above we have

$$\bar{L}'_\Phi e^{\phi'_\mu(x)} + e^{-\phi'_\mu(x)} L'_\Phi = 2\sqrt{L'_\Phi \bar{L}'_\Phi}\cosh(\phi'_\mu(x))\,, \tag{A.17}$$

and thus obtain the probability distribution function for the matter field

$$p'_\Phi(\phi'_\mu(x)) \propto \exp(-2\beta\sqrt{L'_\Phi \bar{L}'_\Phi}\cosh(\phi'_\mu(x)))\,. \tag{A.18}$$

Dropping the primes gives (19). Again, because of $L_\Phi \bar{L}_\Phi = L'_\Phi \bar{L}'_\Phi$, the gauge transformation does not change the variance of the distribution.

References

[1] Louis Bachelier. Théorie de la spéculation. *Annales Scientifiques de l'École Normale Supérieure Sér.*, 3(17):21–86, 1900. Available from: http://www.numdam.org/item?id=ASENS_1900_3_17__21_0.

[2] Robert F. Engle. Autoregressive conditional heteroscedasticity with estimates of variance of united kingdom inflation. *Econometrica*, 50:987–1008, 1982.

[3] Tim Bollerslev. Generalized autoregressive conditional heteroskedasticity. *Journal of Econometrics*, 31(3):307–327, 1986. Available from: http://econpapers.repec.org/RePEc:eee:econom:v:31:y:1986:i:3:p:307-327.

[4] Benoit B. Mandelbrot. The variation of certain speculative prices. *Journal of Business*, 36:394–419, 1963.

[5] Rosario N. Mantegna and H. Eugene Stanley. Scaling behaviour in the dynamics of an economic index. *Nature*, 376:46–49, 1995. doi:10.1038/376046a0.

[6] Rosario N. Mantegna and H. Eugene Stanley. *An introduction to econophysics: correlations and complexity in finance*. Cambridge University Press, New York, 2000.

[7] Thomas Lux and Michele Marchesi. Scaling and criticality in a stochastic multi-agent model of a financial market. *Nature*, pages 498–500, 1999.

[8] B. Dupoyet, H.R. Fiebig, and D.P. Musgrove. Gauge invariant lattice quantum field theory: Implications for statistical properties of high frequency financial markets. *Physica A: Statistical Mechanics and its Applications*, 389(1):107 – 116, 2010. Available from: http://www.sciencedirect.com/science/article/pii/S0378437109007377, doi:DOI:10.1016/j.physa.2009.09.002.

[9] B. Dupoyet, H.R. Fiebig, and D.P. Musgrove. Replicating financial market dynamics with a simple self-organized critical lattice model. *Physica A: Statistical Mechanics and its Applications*, 390(18-19):3120 – 3135, 2011. Available from: http://www.sciencedirect.com/science/article/pii/S0378437111003116, doi:DOI:10.1016/j.physa.2011.04.017.

[10] Kirill Ilinski. *Physics of Finance - Gauge Modelling in Non-equilibrium Pricing*. John Wiley & Sons, New York, 2001.

[11] I. Montvay and G. Münster. *Quantum Fields on the Lattice*. Cambridge University Press, Cambridge, UK, 1994.

[12] M. Creutz. *Quarks, Gluons and Lattices*. Cambridge University Press, 1983.

[13] Joseph L. McCauley. *Dynamics of Markets: The New Financial Economics*. Cambridge University Press, 2nd edition, 2009.

[14] Per Bak and Kim Sneppen. Punctuated equilibrium and criticality in a simple model of evolution. *Phys. Rev. Lett.*, 71(24):4083–4086, Dec 1993. doi:10.1103/PhysRevLett.71.4083.

[15] Per Bak. *How Nature Works: The Science of Self-Organized Criticality*. Copernicus, New York, 1996.

[16] Maya Paczuski, Sergei Maslov, and Per Bak. Avalanche dynamics in evolution, growth, and depinning models. *Phys. Rev. E*, 53(1):414–443, Jan 1996. doi:10.1103/PhysRevE.53.414.

[17] Asger Lunde and Peter R. Hansen. A forecast comparison of volatility models: does anything beat a garch(1,1)? *Journal of Applied Econometrics*, 20(7):873–889, 2005. Available from: http://ideas.repec.org/a/jae/japmet/v20y2005i7p873-889.html.